

Synthesis, Characterization, and in Vitro Evaluation of a Potentially Selective Anticancer, Mixed-Metal [Ruthenium(III)–Platinum(II)] Trinuclear Complex

Amnon Herman,[†] Joseph M. Tanski,[‡] Michael F. Tibbetts,[†] and Craig M. Anderson^{*†}

Departments of Chemistry, Bard College, P.O. Box 5000, Annandale-on-Hudson, New York 12504-5000, and Vassar College, Poughkeepsie, New York 12604

Received December 17, 2006

A new type of mixed-metal trinuclear complex containing platinum(II) and ruthenium(III) fragments that resemble both cisplatin and NAMI-A has been synthesized and characterized by IR, ¹H NMR, elemental analysis, and X-ray crystallography. The water-soluble compound Na₂{*trans,cis,trans*-[Ru^{III}Cl₄(DMSO-*S*)(*μ*-pyz)]₂Pt^{II}Cl₂} (AH-197, pyz = pyrazine) was assessed for its effects on DNA mobility and toxicity against human cancer cell lines. When compared to cisplatin and KP-1019 (which structurally resembles NAMI-A), IC₅₀ results showed that AH-197 had an intermediate toxicity. When this data was coupled with a subsequent COMPARE evaluation (standard COMPARE queries resulted in insignificant correlation coefficients (<0.70) while very low COMPARE correlation coefficients were found in the matrix queries as well), AH-197 yielded a correlation coefficient of 0.19 when compared to cisplatin and 0.25 when compared to KP1019 indicating that AH-197 has a unique behavior.

Introduction

With the discovery of the anticancer properties of *cis*-diamminedichloroplatinum(II), cisplatin (Figure 1),^{1,2} the research of metallopharmaceuticals increased dramatically. Cisplatin is still a widely used anticancer drug and is effective in treating a variety of cancers.³ Cisplatin's cytotoxicity is achieved by forming, mainly, 1,2-intrastrand d(GpG) DNA cross-links. The covalent cross-links cause significant distortion of helical structure and result in inhibition of DNA replication and transcription.^{4,5} The clinical success of cisplatin has proved to be limited due to significant side effects and resistance that cause relapse.³ Therefore, much interest has focused on developing new chemotherapeutic metal complexes with improved properties. Due to the comprehensive studies of cisplatin and insights into its mechanism of interaction with DNA, platinum complexes

have been of initial interest and subsequent study.^{3,6,7,8} Although different platinum-containing complexes have been successfully tested, most of them have been proven to have the same or only slightly better efficacy than cisplatin.³ However, some platinum complexes, such as carboplatin and oxaliplatin, have shown to be active against many types of cancer.^{9,10}

Multinuclear platinum complexes, particularly trinuclear, are one specific class of compounds that have been recently synthesized and have shown to bind to DNA in a manner different from that of cisplatin.^{11–17} These compounds which

* To whom correspondence should be addressed. E-mail: canderso@bard.edu. Phone: 845-758-7293.

[†] Bard College.

[‡] Vassar College.

- (1) Rosenberg, B.; Vancamp, L.; Krigas, T. *Nature* **1965**, *205*, 698–699.
- (2) Rosenberg, B.; Vancamp, L.; Trosko, J. E.; Mansour, V. H. *Nature* **1969**, *222*, 385.
- (3) Zhang, C. X.; Lippard, S. J. *Curr. Opin. Chem. Biol.* **2003**, *7*, 481–489.
- (4) Jamieson, E. R.; Lippard, S. J. *Chem. Rev.* **1999**, *99*, 2467–2498.
- (5) Suo, Z.; Lippard, S. J.; Johnson, K. A. *Biochemistry* **1999**, *38*, 715–726.

- (6) Komeda, S.; Kalayda, G. V.; Lutz, M.; Spek, A. L.; Yamanaka, Y.; Sato, T.; Chikuma, M.; Reedijk, J. *J. Med. Chem.* **2003**, *46*, 1210–1219.
- (7) Komeda, S.; Lutz, M.; Spek, A. L.; Chikuma, M.; Reedijk, J. *Inorg. Chem.* **2000**, *39*, 4230–4236.
- (8) van Zutphen, S.; Pantoja, E.; Soriano, R.; Soro, C.; Tooke, D. M.; Spek, A. L.; den Dulk, H.; Brouwer, J.; Reedijk, J. *Dalton Trans.* **2006**, 1020–1023.
- (9) Fracasso, P. M.; Blessing, J. A.; Molpus, K. L.; Adler, L. M.; Sorosky, J. I.; Rose, P. G. *Gynecol. Oncol.* **2006**, *103*, 523–526.
- (10) Hah, S. S.; Stivers, K. M.; de Vere, White, R. W.; Henderson, P. T. *Chem. Res. Toxicol.* **2006**, *19*, 622–626.
- (11) Qu, Y.; Appleton, T. G.; Hoeschele, J. D.; Farrell, N. P. *Inorg. Chem.* **1993**, *32*, 2591–2593.
- (12) Davies, M. S.; Thomas, D. S.; Hegmans, A.; Berners-Price, S. J.; Farrell, N. *Inorg. Chem.* **2002**, *41*, 1101–1109.
- (13) Hegmans, A.; Berners-Price, S. J.; Davies, M. S.; Thomas, D. S.; Humphreys, A. S.; Farrell, N. *J. Am. Chem. Soc.* **2004**, *126*, 2166–2180.

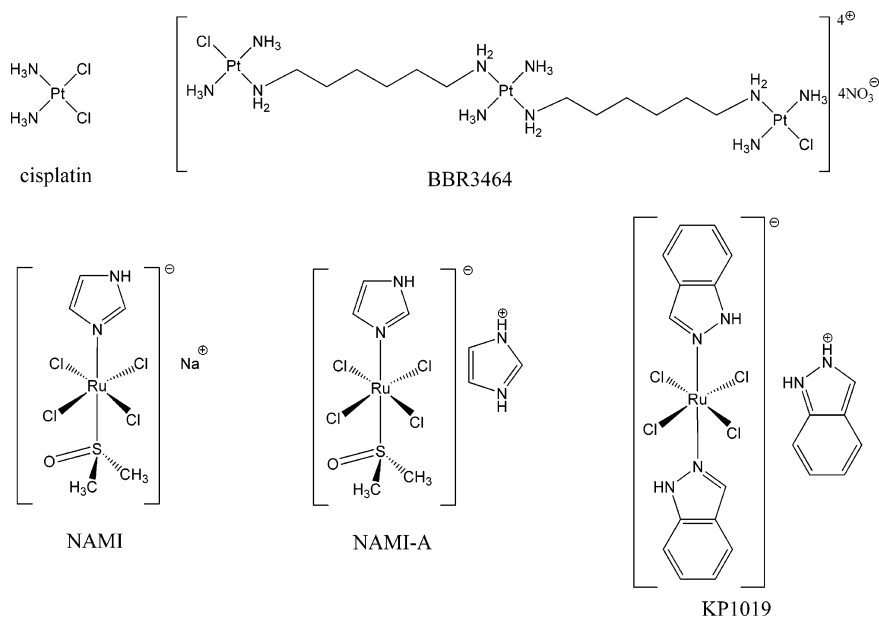


Figure 1. Structures of platinum(II) and ruthenium(III) chemotherapeutic complexes.

contain two or more platinum centers can have both cis and/or trans configurations. BBR3464 (Figure 1) is a representative compound of the polymetallic group which has entered clinical trials and has shown to be potent against pancreatic, lung, and melanoma cancers.^{18,19} It was also found that BBR3464 binds to DNA by forming both intrastrand and interstrand cross-links. Mechanistic studies have shown that the interstrand cross-links, which account for 20% of the cross-link adducts formed by BBR3464, are most important to its anticancer behavior.^{3,20}

For the past two decades much work has focused on the synthesis and pharmacological evaluation of new compounds containing metal centers different from platinum.^{21–23} A major reason for this can be attributed to the reduced side effects of these complexes due to their lower systemic toxicity. Complexes with ruthenium(III) centers have been synthesized and have demonstrated antitumor activity as well as remarkable antimetastatic behavior.^{22,23} It is speculated that ruthenium(III) complexes are reduced in vivo to the more labile ruthenium(II), and this is a major reason for its biological activity.^{21–23} Due to lower oxygen and lower pH

levels at tumor sites, ruthenium's "activation by reduction" process makes it very selective as the metal complex may accumulate in these hypoxic environments.²⁴ Only a small number of ruthenium(III) complexes have been found to be effective with the most prominent examples being the following: Na[*trans*-RuCl₄(DMSO)(Im)],²⁵ NAMI; its more stable imidazolium analogue [ImH][*trans*-RuCl₄(DMSO)(Im)],²⁶ NAMI-A; the closely resembled indazole compound [IndH][*trans*-RuCl₄(Ind)₂],²⁷ KP1019 (Figure 1).

NAMI-A, new antitumor metastasis inhibitor-series A, shows high selectivity for solid tumor metastases^{28,29} and low toxicity at pharmacologically active doses and was found to effectively interfere with cell cycle regulation and angiogenesis.^{30–32} These properties have made NAMI-A the first ruthenium(III) compound to successfully complete phase I clinical trials.³³

In this paper we report the successful modular synthesis of heterotrinnuclear complexes that combine the classes of compounds described above. These compounds have a platinum(II) center that resembles cisplatin as well as two ruthenium(III) centers attached to the platinum by bridging dinitrogen ligands that resemble NAMI. The design of these

- (14) Harris, A. L.; Qu, Y.; Farrell, N. P. *Inorg. Chem.* **2005**, *44*, 1196–1198.
 (15) Harris, A. L.; Yang, X.; Hegmans, A.; Povirk, L.; Ryan, J. J.; Kelland, L.; Farrell, N. P. *Inorg. Chem.* **2005**, *44*, 9598–9600.
 (16) Komeda, S.; Kalayda, G. V.; Lutz, M.; Spek, A. L.; Yamanaka, Y.; Sato, T.; Chikuma, M.; Reedijk, J. *J. Med. Chem.* **2003**, *46*, 1210–1219.
 (17) Komeda, S.; Moulaci, T.; Woods, K. K.; Chikuma, M.; Farrell, N. P.; Williams, L. D. *J. Am. Chem. Soc.* **2006**, ASAP.
 (18) Servidei, T.; Ferlini, C.; Riccardi, A.; Meco, D.; Scambia, G.; Segni, G.; Manzotti, C.; Riccardi, R. *Eur. J. Cancer* **2001**, *37*, 930–938.
 (19) Jodrell, D. I.; Evans, T. R. J.; Steward, W.; Cameron, D.; Prendiville, J.; Aschele, C.; Noberasco, C.; Lind, M.; Carmichael, J.; Dobbs, N.; Camboni, G.; Gatti, B.; De Braud, F. *Eur. J. Cancer* **2004**, *40*, 1872–1877.
 (20) Kasparkova, J.; Zehnulova, J.; Farrell, N.; Brabec, V. *J. Biol. Chem.* **2002**, *277*, 48076–48086.
 (21) Brabec, V.; Novakova, O. *Drug Resist. Updat.* **2006**, *9*, 111–122.
 (22) Alessio, E.; Mestroni, G.; Bergamo, A.; Sava, G. *Met. Ions Biol. Syst.* **2004**, *42*, 323–351.
 (23) Kostova, I. *Curr. Med. Chem.* **2006**, *13*, 1085–1107.

- (24) Clarke, M. J. In *Metal Ions in Biological Systems*; Sigel, A., Sigel, H., Eds.; Marcel Dekker: New York, 1979; pp 231–283.
 (25) Alessio, E.; Balducci, G.; Calligaris, M.; Casta, G.; Attia, W.; Mestroni, G. *Inorg. Chem.* **1991**, *30*, 609–618.
 (26) Mestroni, G.; Alessio, E.; Sava, G. International Patent PCT C 07F 15/00, A61K 31/28, WO 98/00431, 1998.
 (27) Hartinger, C. G.; Zorbas-Seifried, S.; Jakupec, M. A.; Kynast, B.; Zorbas, H.; Keppler, B. K. *J. Inorg. Biochem.* **2006**, *100*, 891–904.
 (28) Cocchietto, M.; Sava, G. *Pharmacol. Toxicol.* **2000**, *87*, 193–197.
 (29) (a) Serli, B.; Iengo, E.; Gianferrara, T.; Zangrando, E.; Alessio, E. *Met.-Based Drugs* **2001**, *8*, 9–18. (b) Zorzet, S.; Sorc, A.; Casarsa, C.; Cocchietto, M.; Sava, G. *Met.-Based Drugs* **2001**, *8*, 1–7.
 (30) Sava, G.; Bergamo, A.; Cocchietto, M. *Clin. Cancer Res.* **2000**, *6*, 4566.
 (31) Sava, G.; Capozzi, I.; Clerici, V.; Gagliardi, G.; Alessio, E.; Mestroni, G. *Clin. Exp. Metastasis* **1998**, *16*, 371–379.
 (32) Clarke, M. J. *Coord. Chem. Rev.* **2003**, *236*, 209–233.
 (33) Rademaker-Lakhai, J. M.; Van den Bongard, D.; Pluim, D.; Beijnen, J. H.; Schellens, J. H. *Clin. Cancer Res.* **2004**, *10*, 3717–3727.

complexes has been done to achieve both efficacy and selectivity with the objective of obtaining complexes with properties of both types of metal complexes. The new type of complex may then be potent against both neoplastic and metastatic cancers. In addition, the ruthenium(III) centers are susceptible to reduction to the more labile ruthenium(II) which may weaken the ruthenium(II)–bridging ligand bonds.³⁴ These trinuclear species may also achieve better selectivity due to the transferrin cycle mediated accumulation of ruthenium(III) compounds in hypoxic environments and subsequent “activation by reduction” of the ruthenium(III) centers in these conditions.²³

The water-soluble trinuclear complex AH-197 was evaluated for its *in vitro* activity with linearized plasmid DNA as well as against the NCI’s 60 human tumor cell line screening procedure and its algorithm, COMPARE.

Experimental Section

cis-PtCl₂(pyz)₂ and [(DMSO)₂H][*trans*-RuCl₄(DMSO)₂] were synthesized by following literature preparations.^{35,25} The sodium, tetrabutylammonium (TBA), and tetraphenylphosphonium (TPP) salts of the [*trans*-RuCl₄(DMSO)₂][−] anion were obtained from simple metathesis reactions.³⁶ Ethanol (200 proof) was purchased from Pharmaco Products Inc. All other reagents and solvents were purchased from Sigma Aldrich Inc. IR spectra were recorded in the solid state on a Nicolet 4700 FTIR spectrometer between 4000 and 250 cm^{−1}. ¹H NMR spectra were measured in D₂O, acetone-*d*₆, CDCl₃, and CD₃CN on a Varian Gemini 300 MHz spectrometer. The solvent peaks at 4.80, 2.05, 7.24, and 1.96 ppm for D₂O, C₂D₆O (acetone), CDCl₃, and CD₃CN, respectively, were used as internal standards for the ¹H NMR spectra. UV/vis were run on an Agilent 8453 diode array instrument. Plasmid’s miniprep extractions as well as purification kits were purchased from Qiagen Inc. IC₅₀ assays were conducted as part of the *in vitro* anticancer screening offered by the Developmental Therapeutic Program in the National Cancer Institute (Bethesda, MD). Detailed experimental procedures for these assays are found online (<http://dtp.nci.nih.gov/branches/btb/ivclsp.html>). Spectral abbreviations used below: br (broad); m (medium); s (strong); sh (shoulder); vbr (very broad); w (weak). For NMR labels see Scheme 1.

Na₂{*trans,cis,trans*-[Ru^{III}Cl₄(DMSO-*S*)(μ-pyz)₂Pt^{II}Cl₂], AH-197. A 0.21 g amount of Na[*trans*-RuCl₄(DMSO)₂] (0.49 mmol) was partially dissolved in 30 mL of acetone, and 0.10 g of *cis*-PtCl₂(pyz)₂ (0.23 mmol) was added *in situ* to the orange suspension. The mixture was then refluxed for 1 h, during which all of the reactants dissolved and the solution turned dark red. The solution was cooled to room temperature. An orange precipitate was afforded by the addition of 10 mL of diethyl ether that was collected by filtration, washed with diethyl ether, and vacuum-dried. A yield of 0.17 g obtained (65%). Selected IR (ν_{max}/cm^{−1}): 1699 m, 1614 m, br (pyz), 1077 s (Ru–DMSO-*S*), 515 m (Pt–N), 429 m (Ru–S), 331 s (Pt/Ru–Cl). ¹H NMR (D₂O): −14.0 br (DMSO-*S*), −2.2 br (pyz H^{2,6}). Anal. Calcd for C₁₂H₂₀Cl₁₀N₄Na₂O₂S₂Ru₂Pt·1/2CH₃COCH₃: C, 14.1; H, 2.01; N, 4.89. Found: C, 13.7; H, 2.08; N, 4.37. Selected UV/vis (PBS): λ_{max}/nm 393 (ε/L mol^{−1} cm^{−1} 11 900); immediately after reduction 478 (11 200).

Complexes with the TPP (AH-166), TBA (AH-171), and imidazolium (AH-235) cations were prepared similarly or by simple metathesis reactions (see Supporting Information).

[TPP]₂{*trans,trans,trans*-[Ru^{III}Cl₄(DMSO-*S*)(μ-pyz)₂Pt^{II}Cl₂], AH-229. A solution of AH-166 was left in acetone solution at 4 °C for 1 month. Dark red crystals appeared very slowly. The crystals were then collected by filtration and washed with ether. Alternatively, [TPP]Cl was mixed with 0.5 equiv of AH-197 and AH-229 was allowed to slowly crystallize over a period of several weeks at −15 °C. Selected IR (ν_{max}/cm^{−1}): 1707 m (pyz), 1106 s (Ru–DMSO-*S*), 521 vs, br (Pt–N), 421 m (Ru–S), 328 s, 307 sh (Pt/Ru–Cl). ¹H NMR (CD₃CN): −1.0 br (pyz H^{2,6}), −12.9 br (DMSO-*S*).

DNA Migration Studies. The plasmid pBluescript SK+ was purified from *Escherichia coli* using a QIAGEN plasmid midi kit as described by the manufacturer (QIAGEN Inc.). Plasmid DNA was linearized with the restriction endonuclease EcoRI and purified from the reaction with a QIAquick PCR Purification Kit (QIAGEN Inc.) eluted in deionized water. The procedure used in these studies is a modification of that described by Stellwagen.³⁷ Briefly, 0.5 μg of linearized pBluescript SK+ was incubated with varying concentrations of the metal compounds in phosphate buffered saline, PBS (3.8 mM NaH₂PO₄, 16.2 mM Na₂HPO₄, 150 mM NaCl, pH 6.4), in a total volume of 50 μL at 37 °C for 24 h. Following incubation, 20 μL samples were analyzed by agarose gel electrophoresis (0.9% agarose, 1X TBE (89 mM Tris base, 89 mM boric acid, 3.1 mM EDTA)). Gels were stained with 5 μg/mL ethidium bromide in 1X TBE for 45 min and photographed with UV illumination.

NCI’s 60 Cell *In Vitro* Cancer Screenings. AH-197 was screened against the 60 human cancer cell lines (NCI-60) used by the National Cancer Institute’s Developmental Therapeutics Program (detailed procedure found at <http://dtp.nci.nih.gov/branches/btb/ivclsp.html>). However, AH-197 was dissolved in water, not DMSO, prior to dilution. The pH of the medium used in the procedure was 7.2. Additional evaluation of data from screenings of AH-197 (NSC: 742192) was conducted using the pattern-recognition algorithm COMPARE (<http://itbwork.nci.nih.gov>).³⁸ Standard COMPARE queries were performed against all synthetic compounds in the NCI’s Developmental Therapeutic Program Database (http://dtp.nci.nih.gov/docs/dtp_search.html) to obtain correlation coefficients. Furthermore, matrix COMPARE of our compound was performed against screening data from cisplatin (NSC: 119875) and KP1019 (NSC: 666158).

X-ray Structure Determinations. X-ray diffraction data were collected on a Bruker SMART APEX 2 CCD platform diffractometer (Mo Kα (λ = 0.710 73 Å)). Suitable crystals were mounted in a nylon loop with Paratone-N cryoprotectant oil. The structures were solved using direct methods and standard difference map techniques and were refined by full-matrix least-squares procedures on *F*² with SHELXTL (version 6.14).³⁹ All non-hydrogen atoms were refined anisotropically. Hydrogen atoms were included in calculated positions and were refined using a riding model. Crystal data and refinement details are presented in Table 1.

AH-197. Single crystals of AH-197 were grown from acetone at 4 °C. Several crystals were screened and found to be multiply twinned. X-ray diffraction data were collected at 115 K on a crystal

(34) Clarke, M. J.; Zhu, F.; Frasca, D. R. *Chem. Rev.* **1999**, *99*, 2511–2533.

(35) Foulds, G.; Thornton, D. *Spectrochim. Acta.* **1981**, *37*, 917–921.

(36) (a) Alessio, E.; Bolle, M.; Milani, B.; Mestroni, G.; Faleschini, P.; Geremia, S.; Calligaris, M. *Inorg. Chem.* **1995**, *34*, 4716. (b) Anderson, C. M.; Herman, A.; Rochon, F.D. *Polyhedron*, **2007**, *26*, 3661–3668.

(37) Stellwagen, N. *Nucleic acid electrophoresis*; Springer: Berlin, 1998; pp 1–53.

(38) Boyd, M. R.; Paull, K. D. *Drug. Dev. Res.* **1995**, *34*, 91–109.

(39) Sheldrick, G. M. *SHELXTL, An integrated system for solving, refining and displaying crystal structures from diffraction data*; University of Göttingen: Göttingen, Germany, 1981.

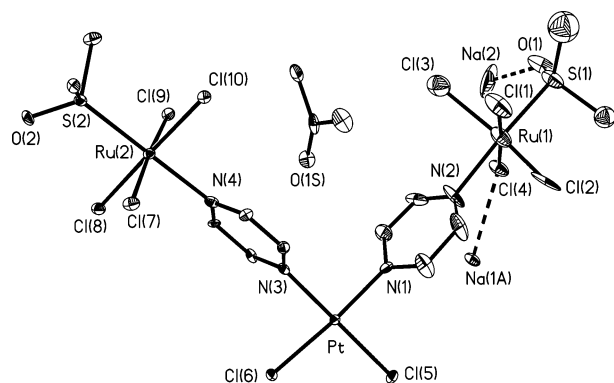


Figure 2. ORTEP diagram of the asymmetric unit of *cis*-AH-197 (20% ellipsoids; hydrogen atoms removed for clarity).

Table 1. Crystal Data, Data Collection, and Refinement Parameters for AH-197 and AH-229

param	<i>cis</i> -AH-197	<i>trans</i> -AH-229
formula	C ₁₂ H ₂₀ Cl ₁₀ N ₄ O ₂ Na ₂ S ₂ Ru ₂ Pt·C ₃ H ₆ O	C ₆₀ H ₆₀ Cl ₁₀ N ₄ O ₂ P ₂ S ₂ Ru ₂ Pt·2C ₃ H ₆ O
habit, color	plate, orange	needle, yellow
size, mm	0.13 × 0.10 × 0.03	0.32 × 0.07 × 0.04
lattice type	triclinic	triclinic
space group	<i>P</i> $\bar{1}$	<i>P</i> $\bar{1}$
<i>a</i> , Å	12.526(2)	14.6756(7)
<i>b</i> , Å	12.667(2)	15.3198(7)
<i>c</i> , Å	17.570(3)	17.0886(8)
α , deg	106.517(2)	76.981(1)
β , deg	95.159(2)	73.257(1)
γ , deg	115.745(2)	84.799(1)
<i>V</i> , Å ³	2332.9(7)	3583.2(3)
<i>Z</i>	2	2
<i>fw</i>	1172.23	1863.07
<i>D_c</i> , g cm ⁻³	1.669	1.727
μ , mm ⁻¹	4.331	2.889
<i>F</i> (000)	1116	1852
θ range, deg	1.68–28.17	1.45–28.52
index ranges	−16 ≤ <i>h</i> ≤ 16, −16 ≤ <i>k</i> ≤ 16, −23 ≤ <i>l</i> ≤ 22	−19 ≤ <i>h</i> ≤ 19, −19 ≤ <i>k</i> ≤ 19, −22 ≤ <i>l</i> ≤ 22
reflens collcd	50 545	42 414
unique reflens	10 350 (<i>R</i> _{int} = 0.0928)	16 490 (<i>R</i> _{int} = 0.0497)
completeness	90.4 (to Φ = 28.17°)	90.6 (to Φ = 28.52°)
abs corr	empirical	empirical
max, min transm	0.8810, 0.6029	0.9056, 0.4583
data, restraints, params	33 000/33/350	16 490/0/793
<i>R</i> ₁ , <i>wR</i> ₂ (<i>I</i> > 2 σ (<i>I</i>))	0.1045, 0.2570	0.0377, 0.0620
<i>R</i> ₁ , <i>wR</i> ₂ (all data)	0.1776, 0.3003	0.0592, 0.0671
goodness-of-fit (on <i>F</i> ²)	1.012	1.009
largest diff peak, hole, e Å ⁻³	8.659, −5.649	1.300, −0.793

that was determined with CELL_NOW to contain two twin domains. Both domains were integrated with SAINT using the two-component orientation matrix produced by CELL_NOW. The data were scaled and absorption corrected with TWINABS. The initial solution was refined with single component data for the stronger domain before final refinement with HKLF 5 format data for both twin domains as produced by TWINABS. An ORTEP diagram of the molecule is shown in Figure 2. Selected bond length and angles are given in Table 2.

AH-229. Suitable X-ray-quality single crystals of AH-229 were grown from acetone at 4 °C. X-ray diffraction data were collected at 125 K. The asymmetric unit contains two unique half-molecules, one from each of the independent trinuclear molecules of AH-229, each platinum atom residing on an inversion center. The unit cell contains four molecules of acetone solvent of crystallization,

Table 2. Selected Bond Lengths (Å) and Angles (deg)^a for AH-197

Pt–N(1)	2.01(1)	N(1)–Pt–N(3)	89.8(4)
Pt–N(3)	2.03(1)	N(1)–Pt–Cl(5)	90.2(3)
Pt–Cl(5)	2.290(3)	N(3)–Pt–Cl(6)	86.4(3)
Pt–Cl(6)	2.293(3)	Cl(5)–Pt–Cl(6)	93.7(1)
Ru(1)–N(2)	2.16(2)	N(2)–Ru(1)–S(1)	175.0(4)
Ru(1)–S(1)	2.305(5)	N(2)–Ru(1)–Cl av	88(6)
Ru(1)–Cl av	2.2(3)	S(1)–Ru(1)–Cl av	92(5)
Ru(2)–N(4)	2.12(1)	N(4)–Ru(2)–S(2)	178.0(3)
Ru(2)–S(2)	2.281(4)	N(4)–Ru(2)–Cl av	89(1)
Ru(2)–Cl av	2.347(7)	S(2)–Ru(2)–Cl av	91(1)

^a Estimated standard deviations in the least significant figure are given in parentheses.

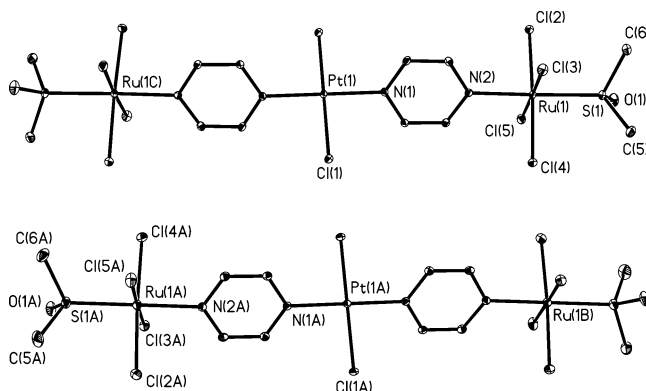


Figure 3. Molecular structures of the two independent molecules of *trans*-AH-229 (20% ellipsoids; hydrogen atoms removed for clarity).

Table 3. Selected Bond Lengths (Å) and Angles (deg)^a for AH-229

Pt(1)–N(1)	2.013(3)	N(1)–Pt(1)–Cl(1)	89.09(9)
Pt(1)–Cl(1)	2.300(1)	N(1#2)–Pt(1)–Cl(1)	90.91(9)
Ru(1)–N(2)	2.101(3)	N(2)–Ru(1)–S(1)	178.52(9)
Ru(1)–S(1)	2.289(1)	N(2)–Ru(1)–Cl av	88.8(3)
Ru(1)–Cl av	2.349(4)	S(1)–Ru(1)–Cl av	91(1)
Pt(1A)–N(1A)	2.024(3)	N(1A)–Pt(1A)–Cl(1A)	90.95(9)
Pt(1A)–Cl(1A)	2.289(1)	N(1A#2)–Pt(1A)–Cl(1A)	89.05(9)
Ru(1A)–N(2A)	2.103(3)	N(2A)–Ru(1A)–S(1A)	178.51(9)
Ru(1A)–S(1A)	2.289(1)	N(2A)–Ru(1A)–Cl av	89(1)
Ru(1A)–Cl av	2.352(17)	S(1A)–Ru(1A)–Cl av	91(1)

^a Estimated standard deviations in the least significant figure are given in parentheses.

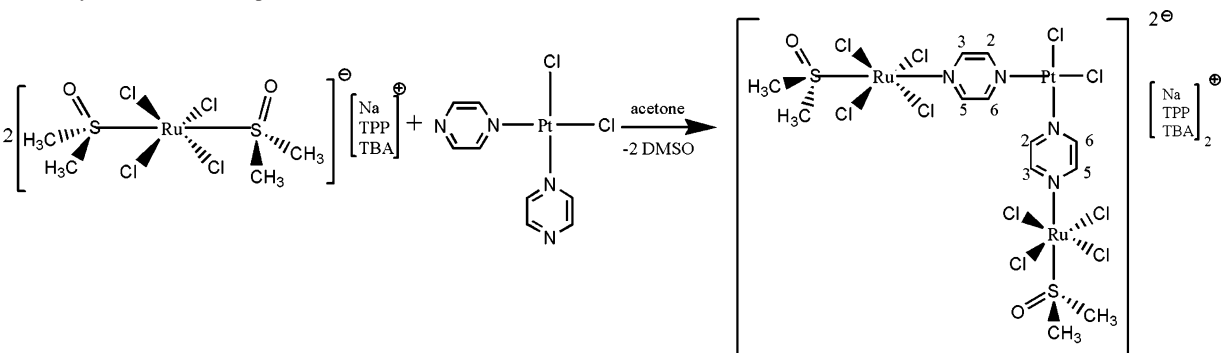
two of which have been located and refined and two of which are disordered. The atoms of the disordered acetone molecules were included in the refinement as a diffuse contribution to the scattering using the program SQUEEZE in the PLATON suite of programs.⁴⁰ ORTEP diagrams of the two independent molecules are shown in Figure 3. Selected bond length and angles are given in Table 3.

Results and Discussion

Synthesis and Characterization of the Complexes. Ruthenium(III) precursors were synthesized by modifications of those reported by Allesio et al.²⁵ [(DMSO)₂H][*trans*-RuCl₄(DMSO)₂], **1**, was the initial ruthenium(III) compound from which the other ruthenium(III) compounds were derived. Complexes with different cations (Na, **2**; TPP, **3**; TBA, **4**) resulted from simple metathesis reactions of **1** with the chloride salts of the appropriate cations (NaCl, TPP-Cl, TBA-Cl) in appropriate molar ratios. The platinum(II) precursor was synthesized according to an earlier report by Foulds et al.³⁵

(40) Spek, A. L. *Acta Crystallogr.* **1990**, *A46*, C34.

Scheme 1. Synthesis of the Complexes



Synthesis of the trinuclear complex AH-197 was achieved by refluxing a mixture of the ruthenium and platinum precursors listed above, in a 2.1:1 ratio, respectively. The initial insoluble nature of the platinum precursor was used as indication for the extent of the reaction; as the platinum complex dissolved and the solution reached homogeneity, the reaction was assumed to be complete. This resulted in the bridging of the pyrazine ligand between the platinum center and the ruthenium center as a result of a substitution of the pyrazine for the DMSO ligand on the ruthenium. The general route is outlined in Scheme 1. The trans isomer of the trinuclear species was obtained from aged solutions of AH-197 in acetone with the addition of the tetraphenylphosphonium cation or from aged solutions of the *cis*-TPP isomer, AH-166. *Cis* chloro/pyridine platinum complexes are known to slowly isomerize to the trans configuration.^{41,42} In addition, computation studies using Gaussian '03⁴³ show the trans isomer of the dianion to be slightly lower in energy than the *cis* dianion (see Supporting Information).

The vibrational spectra for *cis*-PtCl₂(pyz)₂ and [(DMSO)₂H]-[*trans*-RuCl₄(DMSO)₂] have been reported,^{35,25} and the assignments on the platinum(II) and ruthenium(III) fragments of the new complexes are based on these studies. Infrared spectroscopy is diagnostic of the binding mode (terminal or bridging) of coordinated pyrazines.⁴⁴ Monocoordinated pyrazine compounds (terminal) are characterized by a "breathing mode" which gives a sharp peak at about 1590 cm⁻¹.⁴⁵ That peak is absent if pyrazine acts as a bridging ligand

as in complex AH-197. Two new peaks at 1699 and 1615 cm⁻¹ are present in the spectrum of AH-197. The trans complex shows only one peak for the pyrazine mode at 1707 cm⁻¹.

The NMR spectrum of AH-197 (Supporting Information) shows peaks that are characteristic of complexes containing paramagnetic ruthenium(III).^{46,47} Protons close to the paramagnetic center have large line widths (often some peaks are too wide to be observable) and are shifted greatly upfield. The peak at -14.0 ppm integrating to 12 protons is assigned to the coordinated DMSO while the peak at -2.2 ppm integrating to 4 protons is assigned to the protons on the pyrazine ring closest to the platinum center, thus furthest from the paramagnetic ruthenium(III) center. The protons on the pyrazine ring closest to the ruthenium center are not observed (for labeling, see Scheme 1). The proton NMR of the trans complex, AH-229, recorded in CD₃CN showed peaks at -13.2 ppm for the DMSO methyl protons and -1.0 ppm for the pyrazine protons furthest from the ruthenium as well as the phenyl peaks associated with the TPP cation.

The trinuclear complex AH-197 has its ruthenium(III) centers reduced to ruthenium(II) upon the addition of 2 equiv of the biological reductant, ascorbic acid. This was witnessed in both NMR and UV/vis experiments. Upon addition of ascorbic acid to a solution of AH-197, an immediate reaction is seen as the color changes from orange to red. In the UV/vis spectrum, the lowest energy peak at 393 nm shifted to 480 nm upon addition of ascorbic acid as is characteristic of reduction of ruthenium(III) to ruthenium(II).^{29,45} In the NMR spectrum, upon addition of ascorbic acid, there is an immediate and complete disappearance of the peaks associated with the paramagnetic ruthenium(III) species, AH-197, indicating a quantitative reduction of the ruthenium(III). The disappearance of the paramagnetic upfield peaks is accompanied with the appearance of several new, overlapping downfield peaks between 8.6 and 9.6 ppm and 3.4 and 3.6 ppm characteristic of a mixture of a number of possible species including ruthenium(II)/pyrazine(bridging or terminal)/DMSO complexes.^{29,45}

The structures of the *cis* trinuclear complex and of the *trans* trinuclear complex were determined. The bond lengths

(41) Rochon, F. D.; Kong, P. C. *Can. J. Chem.* **1979**, *57*, 526–529.

(42) Rochon, F. D.; Kong, P. C.; Melanson, R. *Can. J. Chem.* **1981**, *59*, 195–198.

(43) Frisch, M. J.; Trucks, G. W.; Schlegel, H. B.; Scuseria, G. E.; Robb, M. A.; Cheeseman, J. R.; Montgomery, J. A., Jr.; Vreven, T.; Kudin, K. N.; Burant, J. C.; Millam, J. M.; Iyengar, S. S.; Tomasi, J.; Barone, V.; Mennucci, B.; Cossi, M.; Scalmani, G.; Rega, N.; Petersson, G. A.; Nakatsuji, H.; Hada, M.; Ehara, M.; Toyota, K.; Fukuda, R.; Hasegawa, J.; Ishida, M.; Nakajima, T.; Honda, Y.; Kitao, O.; Nakai, H.; Klene, M.; Li, X.; Knox, J. E.; Hratchian, H. P.; Cross, J. B.; Bakken, V.; Adamo, C.; Jaramillo, J.; Gomperts, R.; Stratmann, R. E.; Yazyev, O.; Austin, A. J.; Cammi, R.; Pomelli, C.; Ochterski, J. W.; Ayala, P. Y.; Morokuma, K.; Voth, G. A.; Salvador, P.; Dannenberg, J. J.; Zakrzewski, V. G.; Dapprich, S.; Daniels, A. D.; Strain, M. C.; Farkas, O.; Malick, D. K.; Rabuck, A. D.; Raghavachari, K.; Foresman, J. B.; Ortiz, J. V.; Cui, Q.; Baboul, A. G.; Clifford, S.; Cioslowski, J.; Stefanov, B. B.; Liu, G.; Liashenko, A.; Piskorz, P.; Komaromi, I.; Martin, R. L.; Fox, D. J.; Keith, T.; Al-Laham, M. A.; Peng, C. Y.; Nanayakkara, A.; Challacombe, M.; Gill, P. M. W.; Johnson, B.; Chen, W.; Wong, M. W.; Gonzalez, C.; Pople, J. A. *Gaussian '03*; Gaussian, Inc.: Wallingford CT, 2004.

(44) Collman, J. P.; McDevitt, J. T.; Leidner, C. R.; Yee, G. T.; Torrance, J. B.; Little, W. A. *J. Am. Chem. Soc.* **1987**, *109*, 4606–4614.

(45) Allesio, E.; Mestroni, G.; Geremia, S.; Calligaris, M.; Iengo, E. *Dalton Trans.* **1999**, *19*, 3361–3371.

(46) Anderson, C.; Beauchamp, A. L. *Inorg. Chem.* **1995**, *34*, 6065–6073.

(47) Anderson, C. *Can. J. Chem.* **2001**, *79*, 1477–1482.

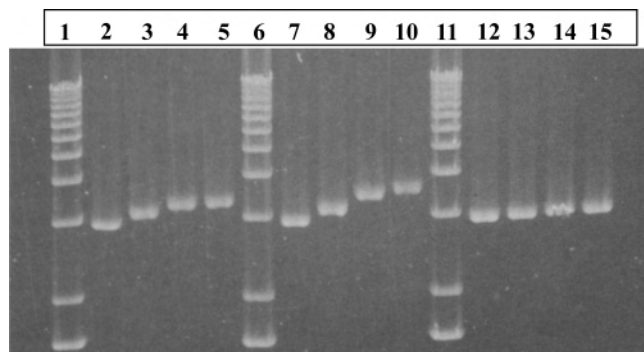


Figure 4. Concentration-dependent interactions of metal complexes with DNA. A total of 0.5 μg of linearized plasmid DNA was incubated with varying concentrations of cisplatin, AH-197, or Na[*trans*-RuCl₄(DMSO)(pyz)], at 37 °C for 24 h. A 1 kb plus molecular weight standard (Invitrogen) was included for reference. Lanes 1, 6, and 11: 1 kb plus DNA ladder. Lanes 2–5: 0, 0.1, 0.5, 1.0 mM cisplatin, respectively. Lanes 7–10: 0, 0.1, 0.5, 1.0 mM AH-197, respectively. Lanes 12–15: 0, 0.1, 0.5, 1.0 mM Na[*trans*-RuCl₄(DMSO)(pyz)], respectively.

and angles for the metal–ligand bonds in the coordination sphere (Tables 2 and 3) are reasonable when compared to similar monomeric and pyrazine-bridged ruthenium(III) and platinum(II) complexes previously reported.^{41,45,48} ORTEP diagrams can be seen in Figures 2 and 3. In the cis complex (AH-197), the angle between the PtCl₂pyz₂ square plane and the plane of the pyz ring is 65.7(5)° for the N1/N2 pyz and 68.8(4)° for the N3/N4 pyz. The trans complex, as stated in the Experimental Section, crystallizes with two independent trinuclear units. In this complex, the angle between the PtCl₂pyz₂ square plane and the plane of the pyz ring is 52.1(1)° for the Pt1 molecule and 40.9(1)° for the Pt1A molecule. This is the principal difference between the two independent molecules in this structure. The larger values for the angles on the cis complex are most probably due to steric hindrance between the pyrazine groups.⁴⁹ Also, when considering the N–Ru–Cl and S–Ru–Cl angles (Tables 2 and 3), it appears that the chlorides cant slightly toward the pyrazine ring and away from the DMSO ligand in each of the cis and the trans complexes.

DNA Migration Studies. Cisplatin is known to form intrastrand cross-links with guanine bases and bend DNA thereby reducing its electrophoretic mobility.^{4,50,51,52} The concentration dependent inhibition of DNA migration due to incubation with AH-197 is shown in Figure 4, suggesting it tightly binds to DNA. To provide a basis for comparison, incubation of DNA with cisplatin and Na[*trans*-RuCl₄(DMSO)(pyz)] was also performed using the same concentrations and conditions. Interestingly, AH-197 appears to have a greater effect on mobility than cisplatin at comparable concentrations (compare Figure 4 lanes 3–5 with lanes 8–10) perhaps reflecting the greater size of AH-197. Not surprisingly, Na[*trans*-RuCl₄(DMSO)(pyz)] appears to show

Table 4. IC₅₀ Values (μM) for AH-197, Cisplatin, and KP1019 for Selected Cell Lines

cell line	AH-197	cisplatin	KP1019
CCRF-CEM (leukemia)	4.3	4.8	24.9
HOP-62 (NSC lung)	5.0	4.5	100
BT-549 (breast)	14.4	14.8	59.8
HT29 (colon)	18.8	27.4	17.4
COLO 205 (colon)	5.5	56.0	53.6

no effect on the electrophoretic mobility of the plasmid (Figure 4 lanes 12–15). Similar ruthenium(III)/DMSO-containing compounds are hypothesized to act on tumor cells through a different mechanism than cisplatin, not necessarily involving DNA binding.^{32,53}

NCI's 60 Cell in Vitro Cancer Screenings. AH-197 was accepted to the NCI's Developmental Therapeutics Program in vitro screening. A general comparison of the IC₅₀ values for the NCI-60 cell lines for AH-197, cisplatin, and KP1019 revealed that AH-197 has an intermediate cytotoxicity compared to the other two compounds (Supporting Information). IC₅₀ values for selected cell lines that show interesting results are presented in Table 4. As shown, AH-197 and cisplatin were almost equally effective in CCRF-CEM leukemia cells (IC₅₀ = 4.3 and 4.8 μM , respectively), HOP-62 NSC lung cells (IC₅₀ = 5.0 and 4.5 μM , respectively), and BT-549 breast cells (IC₅₀ = 14.4 and 14.8 μM , respectively). The IC₅₀ results for KP1019 in HT29 colorectal cells, where efficacy of this compound exceeded cisplatin, led KP1019 to clinical trials as a colorectal chemotherapeutic drug.⁵⁴ The IC₅₀ value for AH-197 in HT29 colorectal cells was similar to that for KP1019. Most interesting was the dissimilar result shown for another colon cancer cell line, COLO 205, for which AH-197 was found to be much more potent in inhibiting cell growth in this cell line than either cisplatin or KP1019.

The computerized, pattern-recognition algorithm, COMPARE, that was developed at the NCI was shown to correlate biochemical mechanisms of action on the basis of the profile of cell sensitivities produced from the screenings^{55,56} and enables the evaluation and exploitation of data from all NCI in vitro screenings. The profile for AH-197 was compared to all synthetic compounds (standard COMPARE) as well as to both cisplatin and KP1019 (matrix COMPARE). Standard COMPARE queries resulted in insignificant correlation coefficients (<0.70, data not shown). Additionally, very low COMPARE correlation coefficients were found in the matrix queries; AH-197 yielded a correlation coefficient of 0.19 when compared to cisplatin and 0.25 when compared to KP1019 (0.0–1.0 range). The low COMPARE

(48) Tessier, C.; Rochon, F. D. *Inorg. Chim. Acta* **1999**, 295, 25–38.
 (49) Rochon, F. D.; Priqueler, J. R. L. *Can. J. Chem.* **2004**, 82, 649–658.
 (50) Flores, A.; Pérez, J. M. *Toxicol. Appl. Pharmacol.* **2001**, 161, 75–81.
 (51) Williams, R. L.; Toft, H. N.; Winkel, B.; Brewer, K. J. *Inorg. Chem.* **2003**, 42, 4394–4400.
 (52) Miao, R.; Mongelli, M. T.; Zigler, D. F.; Winkel, B. S. J.; Brewer, K. J. *Inorg. Chem.* **2006**, ASAP.

(53) Grguric-Sipka, S. R.; Vilaplana, R. A.; Pérez, J. M.; Fuertes, M. A.; Alonso, C.; Alvarez, Y.; Sabo, T. J.; González-Vilchez, F. *J. Inorg. Biochem.* **2003**, 97, 215–220.
 (54) Kapitza, S.; Pongratz, M.; Jakupec, M. A.; Heffeter, P.; Berger, W.; Lackinger, L.; Keppler, B. K.; Marian, B. *J. Cancer Res. Clin. Oncol.* **2005**, 131, 101–110.
 (55) Boyd, R. In *Current Therapy in Oncology*; Niederhuber, J. E., Ed.; BC Decker, Inc.: Philadelphia, PA, 1993; pp 11–22.
 (56) Paull, K. D.; Hamel, E.; Malspeis, L. In *Cancer Chemotherapeutic Agents*; Foye, W. O., Ed.; American Chemical Society: Washington, DC, 1995.

coefficients suggest that AH-197 does indeed have a unique profile of tumor cell sensitivities and therefore it is likely that AH-197 has a novel biological mechanism of action.⁵⁶

Like NAMI-A, AH-197 failed the usual in vitro screenings such as the NCI's due to low overall toxicity to the cancer cell lines. It is well-established that ruthenium(III) compounds are not toxic compared to platinum complexes and hence do not yield the required IC₅₀ values.⁵⁷ One reason for the low values may be the failure of the in vitro screenings to mimic the reduction potential that is found in the in vivo cancer environments. Nevertheless, both NAMI-A and KP1019 showed good results in treating cancer in vivo and this led them to clinical trials.^{27,33} AH-197 generally showed intermediate IC₅₀ values between those of KP1019 and cisplatin. Given the above and our knowledge of NAMI-A and KP1019, leads us to conclude that, generally, the cytotoxicity of AH-197 is due to the activity of the platinum center. Tumor environment has been found to be acidic and be favorable for the reduction of ruthenium(III) to ruthenium(II).⁵⁸ Under such conditions KP1019 and NAMI-A were found to respond differently; a chloride ligand is the first ligand of KP1019 to hydrolyze upon reduction, whereas, for NAMI-A, the imidazole ligand trans to DMSO is the first to hydrolyze.^{58,59} Therefore, upon reduction, AH-197 might fragment into one platinum(II) and two ruthenium(II) centers, which could result in better inhibition of cell growth exerted by the cisplatin-like moiety while the two ruthenium(II) centers could follow NAMI-A-like behavior and reduce metastasis. Another possible advantage of combining the ruthenium(III) and platinum(II) moieties stems from data of in vitro and in vivo reactions of these fragments with serum proteins such as albumin and transferrin.^{60,61} In these studies, ruthenium and platinum compounds were found to compete with iron for the binding sites of transferrin. The high demand for iron in cancer cells, which results in high expression of transferrin receptors in these cells, may lead to accumulation of ruthenium and platinum compounds in the tumor environment.^{61–63} Hence, the different reactivity of cisplatin, NAMI-A, and KP1019 with these proteins are

important when evaluating a modular compound such as AH-197. Large proportions of cisplatin has been found to bind irreversibly to albumin and transferrin and thereby lose much of its antitumor activity while NAMI-A and KP1019 were found to bind reversibly to these proteins and retain their heterocyclic ligands.^{23,60,61} Therefore, AH-197, which may have restricted binding properties for its platinum center due to the attached ruthenium moieties, could well achieve better efficacy in its delivery to the tumor site. Recent combination therapy results using both cisplatin and NAMI-A on lung metastasis mouse models revealed an exceptional activity; more than 60% of the animals were cured of the cancer.^{57,60}

Concluding Remarks. AH-197 showed interesting behavior under our experimental conditions. AH-197 is quickly and quantitatively reduced by ascorbic acid; therefore, the compound may be activated by reduction as expected for ruthenium(III) compounds. The hybrid (cisplatin–NAMI) nature of our compound allows for the potential of combined efficiency of mechanisms and, perhaps, higher selectivity against both neoplastic tumors and metastatic cancer. Although AH-197 was not chosen for continued studies by the NCI due only to its lack of overall cytotoxicity, this is not a grave concern. It has been very recently reported, for several reasons, that the existing screening procedures are in need of updating as many of the most promising new pharmaceuticals have “failed” the NCI screening which does not account for the possible in vivo activity of weakly cytotoxic drugs.^{57,64} We look forward to further testing of our new class of compounds and the related analogues that we are preparing.

Acknowledgment. We thank Bard College, Vassar College, and The National Science Foundation (Grant NSF 0521237 to J.M.T. (PI) and C.M.A.) for generous financial support. We thank the Developmental Therapeutic Program in the National Cancer Institute for accepting our compound for cancer in vitro screenings. We thank Skylar Ferrara for his valuable discussions. We thank James Morris for help with the computations studies.

Supporting Information Available: Tables of IC₅₀ values, syntheses of analogous complexes, CIF files for each structure, and calculated optimized molecular geometries of AH-197 and AH-229 as well as total and zero point energies. This material is available free of charge via the Internet at <http://pubs.acs.org>. CCDC 662891 for AH-197 and CCDC 662892 for AH-229 are available at www.ccdc.cam.ac.uk/data_request/cif.

IC062419H

(64) Deubel, D. V.; Lau, J. K. *Chem. Commun.* **2006**, 2451–2453.

- (57) Dyson, P. J.; Sava, G. *Dalton Trans.* **2006**, 16, 1929–1933.
 (58) Ravera, M.; Cassino, C.; Baracco, S.; Osella, D. *Eur. J. Inorg. Chem.* **2006**, 4, 740–746.
 (59) Ravera, M.; Baracco, S.; Cassino, C.; Zanello, P.; Osella, D. *Dalton Trans.* **2004**, 2347–2351.
 (60) Khalaila, I.; Bergamo, A.; Bussy, F.; Sava, G.; Dyson, P. J. *Int. J. Oncol.* **2006**, 29, 261–268.
 (61) Kratz, F.; Hartmann, M.; Keppler, B.; Mess, L. *J. Biol. Chem.* **1994**, 269, 2681–2688.
 (62) Cazzola, M.; Bergamaschi, G.; Dezza, L.; Arosio, P. *Blood* **1990**, 75, 1903–1919.
 (63) Smith C. A.; Sutherland-Smith, A. J.; Kratz, F.; Baker, E. N.; Keppler, B. K. *J. Biol. Inorg. Chem.* **1996**, 424–431.